Engineering and Technology Journal

Experimental and theoretical study to improve heat transfer using nanofluids flow in copper tube

Check for updates

Zahraa N. Hussain[a]*, **Jamal M. Ali**[a] , **Hasan S. Majdi**[b] , **Abbas J. Sultan**[a] , **Bashar J. Kadhim**[a] , **Haidar Al-Naseri**[c]

[a] Chemical Engineering Dept., University of Technology-Iraq, Alsina'a street, 10066 Baghdad, Iraq.
[b] Chemical Engineering and Petroleum Industries Dept., College of Engineering, Al-Mustaqbal University, Babylon 51001, Iraq.
[c] Chemical Engineering Dept., College of Engineering, Tikrit University, Tikrit, Iraq.
*Corresponding author Email: che.21.01@grad.uotechnology.edu.iq

H I G H L I G H T S

- Explores the integration of TiO_2, CuO, and GNP nanoparticles into base fluids to enhance heat transfer efficiency.
- Experimental and numerical approaches were used to study convective heat transfer under a turbulent flow regime.
- Advanced measurement techniques, including Flux Teq LLC heat flux sensors.
- Nanoparticles in heat transfer fluids improved thermal conductivity and convective heat transfer coefficients.
- The use of nanoparticles reduced energy consumption, enhanced system efficiency, and optimized heat exchange performance

A B S T R A C T

Improving heat transfer efficiency in base fluids remains a key challenge in various thermal applications. To address this, several researchers have suggested the integration of nanoparticles into base fluids, leveraging recent advancements in nanotechnology to enhance performance. This study compares different types of nanoparticles and preparation methods for nanofluids and examines the impact of their properties on improving heat transfer. The convective heat transfer under a turbulent flow regime was studied experimentally and numerically in a copper tube used as a test section. Advanced measurement techniques were employed, including a Flux Teq LLC heat flux sensor mounted on the test section wall's inner surface to measure the instantaneous heat flux and inner surface temperature. Additionally, five T-type thermocouples were used to measure the bulk temperature. Three types of nanoparticles—titanium dioxide, copper oxide, and graphene nanoplates were used at three different concentrations (0.01, 0.02, and 0.03 vol. %) to prepare the nanofluids. The results of applying these nanofluids in the heat transfer process showed that the heat transfer coefficient increased with the concentration of nanoparticles. The greatest improvement was observed at a concentration of 0.03%, with heat transfer coefficient increases compared to the base fluid of 23.7%, 39.1%, and 68.25% for TiO_2, CuO, and GNP, respectively. Numerical results were obtained using COMSOL 5.6, a computational fluid dynamics (CFD) analytical program. The predicted and experimental values were compared to validate the model, showing good agreement between the results, though minor differences were observed. These findings highlight the potential of nanofluids as an innovative solution for advanced heat transfer applications, offering enhanced performance and energy savings.

1. Introduction

Nanotechnology is widely used in many areas of modern life, where adding nanoparticles with sizes less than 100 nm to fluids helps improve heat transfer properties. This method improves the physical and thermal properties of fluids. Many studies worldwide have investigated the possibility of using nanofluids in various applications and equipment. The increasing demand for energy efficiency and improved heat transfer in various industrial applications, such as heat exchangers, cooling systems, and thermal management devices, has led to a great interest in developing advanced heat transfer fluids. The incorporation of nanoparticles into the base fluid, such as water, oil, or ethylene glycol, has been shown to improve heat transfer properties beyond what can be achieved by conventional fluids, making nanofluids an attractive option for a variety of engineering applications [1-3].

Among the various heat transfer methods, convective heat transfer in pipes and tubes under turbulent flow conditions is of utmost importance in industrial heat exchangers, cooling systems, and nuclear reactors. In turbulent flow, the fluid motion is chaotic, which enhances the convective heat transfer coefficient due to the increased mixing and disintegration of thermal boundary layers. However, further enhancement of heat transfer in turbulent flow remains a challenge, which is where nanofluids come into play. The presence of nanoparticles significantly changes the thermophysical properties of the fluid, such as thermal conductivity, viscosity, and specific heat capacity, resulting in improved heat transfer performance [4,5].

Natural convection heat transfer plays a significant role in electronic and mechanical engineering systems, particularly for cooling and heating purposes. Energy conservation during heat transfer in these systems is a critical consideration. Numerous experiments have been conducted in existing literature to improve heat transfer rates using conventional fluids or solids individually. Solids generally have higher thermal conductivity compared to fluids. For instance, the thermal conductivity of zinc oxide exceeds that of typical fluids such as water or engine oil [6]. A nanofluid is a stable combination of conventional fluid and nanoparticles. The enhancement of heat transfer using nanofluids is influenced by factors such as the geometry filled with nanofluid, the combination of base fluid and nanoparticles, high thermal conductivity, minimal resistance to fluid flow, as well as the longevity, stability, and uniformity of the nanoparticles [7,8]. Studies on heat transfer enhancement using graphene nanosheets (GNPs), titanium dioxide (TiO_2), and copper oxide (CuO) have received significant attention in recent years. These nanofluids are promising due to their improved thermal properties and ability to improve heat transfer performance compared to conventional fluids [9,10].

Doshmanziari et al. [11], carried out both experimental and numerical studies to examine the heat transfer and flow characteristics of Al_2O_3/water nanofluid at particle volume concentrations of 0.5%, 1%, and 1.5% in a turbulent flow regime within a spiral-coil tube. The findings revealed that the convective heat transfer coefficient of the nanofluid increased by up to 61% compared to that of the base fluid. A comparison between the simulation results and experimental measurements demonstrated an 85% agreement between the results. Mohammed et al. [12], experimentally and numerically investigated the forced convection heat transfer and pressure drop in spirally coiled tubes using a TiO_2 /water nanofluid as a working fluid. The aim was to investigate and shed more light on how physical and geometric characteristics affect the pressure drop and heat transfer enhancement in spirally coiled tubes. The studies were conducted at nanoparticle concentrations of 0.1, 0.2, and 0.5% for five distinct curvature ratios and in the Reynolds number range of 3000 to 18000. The working fluid's thermophysical characteristics were taken to be a function of the concentration and temperature of the nanofluid in the numerical simulation. Shafiee et al. [13], focused on the heat transfer performance of water-based nanofluids with copper oxide, titanium oxide, and aluminum oxide nanoparticles under turbulent flow in a horizontal tube. Their experimental results indicated that the copper oxide nanofluids showed the highest improvement in heat transfer, with improvements up to 80% at higher nanoparticle concentrations. The study also compared the heat transfer performance with different turbulence models in numerical simulations. Majdi et al. [14], conducted experimental and numerical studies to improve heat transfer using Al_2O_3/water nanofluid in a double-pipe heat exchanger under turbulent flow conditions. The simulation tool utilized was COMSOL Multiphysics. Experimental findings indicated that heat transfer enhancement through both circular fins and nanofluid demonstrated a rise with increasing Reynolds number and nanofluid concentration. Simulation outcomes exhibited a satisfactory alignment with the experimental results of the heat transfer coefficient.

It is evident from the literature analysis above that modeling and simulation are difficult fields that can be utilized to save money and time when compared to conventional experimental methods. The current work will use COMSOL to display the temperature in a copper tube with isothermal boundary conditions using nanofluids based on experimental findings. This work sheds further light on how various nanoparticles, including TiO_2, CuO, and GNP, impact turbulent flow on heat transmission in a copper pipe. This study also examines the physical properties of nanofluids and their impact on improving heat transfer efficiency. Concerning practical applications in industries such as heat exchangers, heat pipes, solar collectors, automobile cooling systems, air conditioning, and heat sinks, this study primarily investigates convective heat transfer employing these nanofluids in a copper tube.

The experimental setup uses advanced measurement techniques, including a heat flux sensor and thermocouples, to collect accurate temperature and heat flux change data. Computational fluid dynamics (CFD) simulations using COMSOL 5.6 will validate the experimental results and model the heat transfer behavior of nanofluids in a turbulent flow. The results of this research are expected to provide valuable insights into the feasibility of using nanofluids as an effective heat transfer medium, contributing to the development of more energy-efficient systems in various engineering applications, such as thermal management in electronics, automotive refrigeration, and industrial heat exchangers.

2. Experimental study

2.1 Preparation of nanofluid

In this study, the nanoparticles used are TiO_2, CuO, and GNP, with average diameters of 50 nm, 30 nm, and 10 nm, respectively, sourced from Sky Spring Nanomaterials (Houston, USA). The thermophysical properties of these nanoparticles are provided in Table 1. Also, characterization analysis was carried out using a Scanning Electron Microscope (SEM) at (the Department of Materials Research, Ministry of Science and Technology in Baghdad). SEM was used to evaluate the morphological specifications of (TiO_2, CuO, and GNP). To prepare the nanofluids, nanoparticles are first mixed with distilled water, the base fluid, at three different concentrations of 0.01%, 0.02%, and 0.03%. A hot plate magnetic stirrer (Model\ HS-860, with a temperature range of 30-300°C) is employed to stir the mixture for four hours, ensuring thorough dispersion and uniform distribution of the particles within the fluid. After this initial stirring, the mixture undergoes an additional process of

ultrasonic treatment for one hour using an ultrasonic bath (Model\ El-5LH, Temperature 40°C, Frequency 20 kHz, Capacity 3.5 L) to promote homogeneity further and achieve the desired nanoparticle volume fraction. Figure 1 illustrates the preparation process of the nanofluid.

Table 1: properties of nanoparticles [15,16,17]

Properties	TiO₂	CuO	GNP
Diameter of particles (nm)	50	30	10
Density (kg/m^3)	3845	6489	2002
Thermal conductivity(w/m.k)	11.7	78	3000
Specific heat capacity (J/kg.**K**)	715	560	943
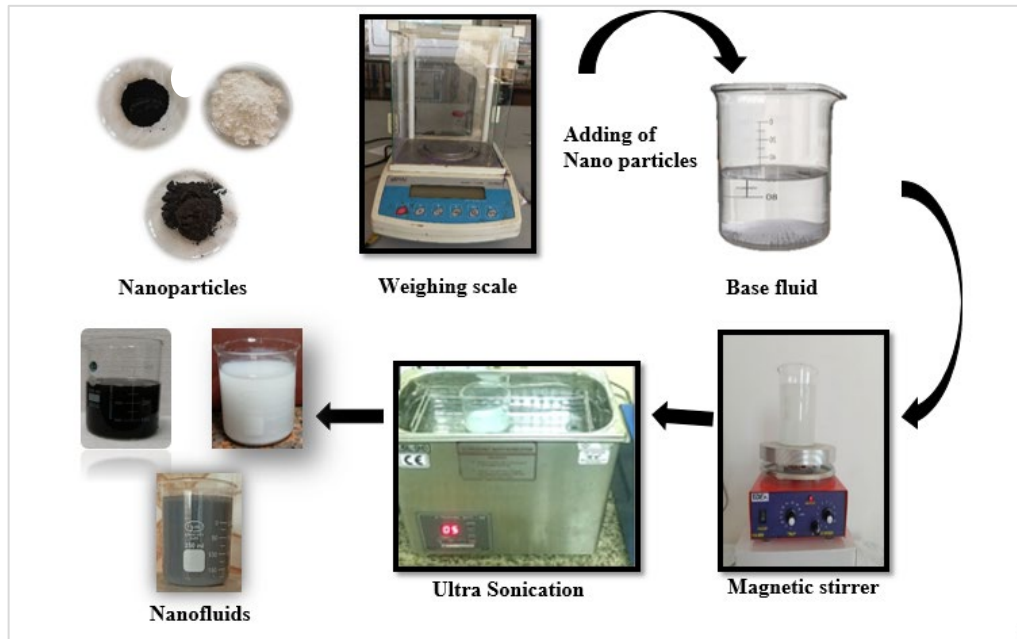
Figure 1: Steps of preparation of nanofluids samples

2.2 Thermophysical properties of nanofluid

When formulating a mathematical model to determine the heat transfer coefficient in forced convection, several fundamental factors must be considered. These factors include fluid properties (such as density, viscosity, and thermal conductivity), fluid flow characteristics (including velocity and turbulence), geometry, and surface conditions of the solid. The density, specific heat capacity, viscosity, and thermal conductivity decided as recommended by Pak and Cho [17], for nanofluid.

Density:

$$\rho_{nf} = (1 - \emptyset)\rho_{bf} + \emptyset\rho_p \tag{1}$$

Specific heat

$$Cp_{nf} = \frac{\emptyset(\rho C_p)_p + (1-\emptyset)(\rho C_p)_{bf}}{\rho_{nf}} \tag{2}$$

Thermal conductivity:

$$k_{nf} = \left[\frac{k_p + 2k_{bf} + 2(k_p - k_{bf})\emptyset}{k_p + 2k_{bf} - 2(k_p - k_{bf})\emptyset}\right] k_{bf} \tag{3}$$

Viscosity:

$$\mu_{nf} = \mu_{bf}(1 + 2.5\emptyset) \tag{4}$$

2.3 Experimental setup

Figure 2 illustrates the schematic diagram of the experimental setup. The setup features a copper test section chosen for its advantageous properties like excellent thermal conductivity, smooth surface, and high hardness. Surrounding the test section is a 60 mm thick ceramic fiber cover with a thermal conductivity of 0.075 W/mK, designed to reduce environmental heat loss.

The apparatus consists of a closed-loop flow system with a 200 cm long pipe, having an inner diameter of 3 cm and an outer diameter of 3.5 cm. It also includes a storage tank and a mixer. The flow rate of the working fluids is adjustable via a bypass regulator. A digital flow meter, located before the test section's inlet, measures the flow rate, which ranges from 1 to 35 liters per minute. Two adjustable valves regulate the flow rate—one in the main flow loop and the other in the bypass line. Pressure measuring devices are positioned at the inlet and outlet of the test section to determine the pressure drop. In addition, the heating unit (consists of a heater, a controller, and a DC power supply). The test section has five T-type thermocouples, which measure the bulk temperature of the liquid, and the FluxTeq LLC (heat flux sensor, VA24060-6370, and Blacksburg, USA), which is attached to the inner surface of the test tube wall using high-temperature glue. A fast response time of approximately 0.6 seconds and a high thermal resistance of 1.0 K/W characterize it. HFS measures the sensor's surface temperature and the local heat flow between the sensor and the bulk fluid. The test section surface is heated using a heater (manufactured by HTS/Amptek Company, made in the USA) to provide the heat through the sensor.
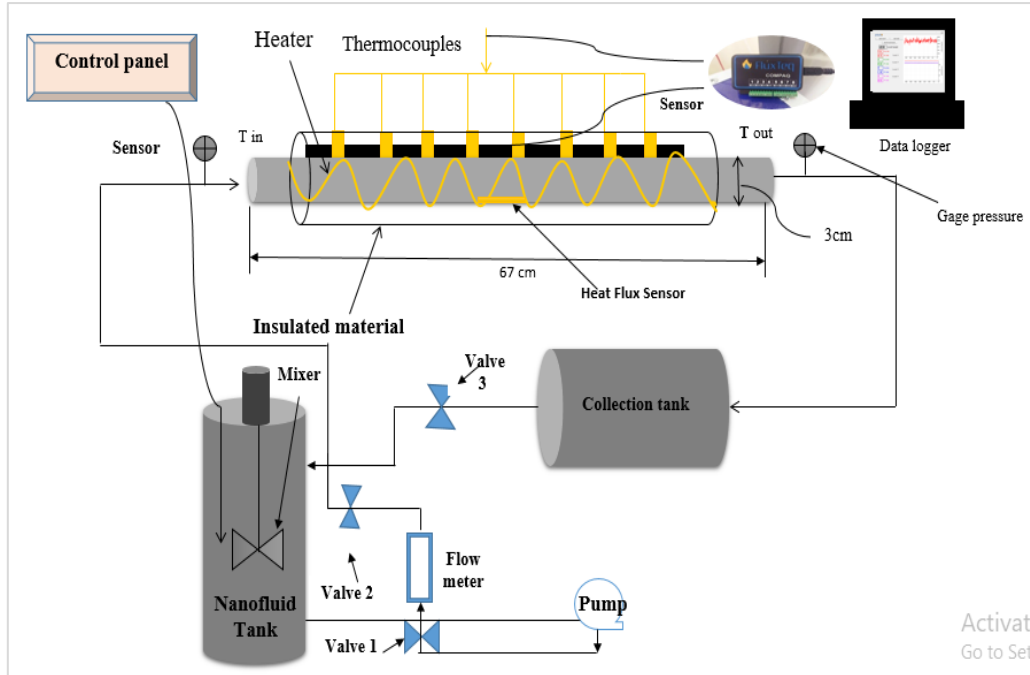

Figure 2: Schematic diagram of an experimental setup

2.4 Data analysis

The heat tube's area was computed as:

$$A = \pi d^2 L \tag{5}$$

The heat flux has been calculated by [18]:

$$q = h\,(T_s - T_b) \tag{6}$$

(h): Heat transfer coefficient $(W/m^2.k)$, q_{conv}: Flow of a heat flux, T_s: Temperature of the surface, T_b: Bulk temperature.

$$T_b = \frac{T_{b1} + T_{b2} + T_{b3} + T_{b4} + T_{b5}}{5} \tag{7}$$

The Nusselt number relationship establishes a mathematical relationship that relates the heat transfer coefficient (h) to the Nusselt number (Nu), the Reynolds number (Re), and the Prandtl number (Pr). The Nusselt number indicates the ratio of convective heat transfer to conductive heat transfer through a surface and is defined as [19,20]:
    Nussle number:

$$Nu = \frac{hd}{k} \tag{8}$$

where, Nu: Nusselt number, h: heat transfer convective, d: diameter of the surface.
    Reynolds number:

$$Re = \frac{\rho u_m d}{\mu} \tag{9}$$

where, Re: Reynold number, ρ: density, u_m: mean velocity, d: diameter of the surface, μ: Viscosity.
Prandtl number:

$$Pr = \frac{c_p \mu}{k} \tag{10}$$

where, Pr: Prandtl number, c_p: specific heat capacity, μ: Viscosity, k: thermal conductivity.
By measuring pressure drop, the friction factor is calculated by Equation (11):

$$f = \frac{\Delta P}{(\frac{L}{D})(\frac{\rho V^2}{2})} \tag{11}$$

3. Computational fluid dynamic

This study used the Computational fluid dynamic (CFD) simulation of 2D using the COMSOL Multiphasic CFD package for a selected condition to predict the temperature profile, velocity distribution, and average surface temperature. These were achieved in the presence and absence of nanofluid for smooth pipe surfaces in turbulent conditions. Then, the COMSOL was simulated to solve the continuity, momentum, and energy equation for the system to predict the temperature and velocity distribution.

4. Numerical simulation

Numerical simulations are conducted to investigate convection heat transfer in a two-dimensional copper tube with fluid flowing through it. The non-dimensional parameters used in this study are the Rayleigh number (Ra), which ranged from 2500 to 5500, and the solid volume fraction ($\emptyset$), which ranged from 0.01 to 0.03. The nanofluids chosen in this study are TiO₂/water, CuO/water, and GNP/water. The geometrical construction of the tube used in the present model is shown in Figure 3.
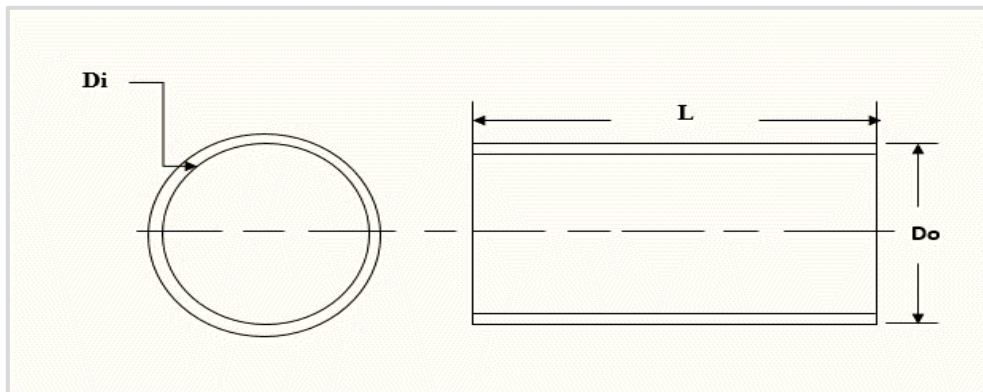

Figure 3: Geometrical dimensions of the tube

The assumptions applied to the governing equations for convective heat transfer in the system where nanofluid flows within a tube are outlined as follows:
1. Steady state.
2. Turbulent single-phase flow (Homogenous model).
3. The base fluid and nanofluid are assumed to be Newtonian, incompressible, and fully developed flow through the system.
4. The effective thermophysical properties are assumed to depend on the nanomaterials' concentration and temperature. In addition, the nanomaterials are tiny with no slip effects.
5. The pressure difference is a driving force in the model.

Based on the assumptions mentioned earlier, the governing equations for the two-phase mixture model can be formulated as:

For steady-state 2D axisymmetric geometries, the expression of continuity is stated as [18]:

$$\frac{\partial}{\partial r}(\rho v_r) + \frac{\partial}{\partial x}(\rho v_x) + \frac{\rho v_r}{r} \tag{12}$$

For each layer, there are two-component of momentum equations; the axial and radial momentum conservation expression is as follows:
Radial- Component

$$\rho_{nf}\left(v_r \frac{\partial v_r}{\partial r} + v_z \frac{\partial v_r}{\partial z}\right) = -\frac{1}{r}\frac{\partial P}{\partial r} + \mu_{nf}\left(\frac{1}{r}\frac{\partial}{\partial r}\left(r\frac{\partial v_r}{\partial r}\right) + \frac{\partial^2 v_r}{\partial z^2} - \frac{v_r}{r^2}\right) \qquad (13)$$

Axial- Component

$$\rho_{nf}\left(v_r \frac{\partial v_z}{\partial r} + v_z \frac{\partial v_z}{\partial z}\right) = -\frac{1}{r}\frac{\partial P}{\partial z} + \mu_{nf}\left(\frac{1}{r}\frac{\partial}{\partial r}\left(r\frac{\partial v_z}{\partial r}\right) + \frac{\partial^2 v_z}{\partial z^2}\right) \qquad (14)$$

The energy equation in the cylindrical coordinates takes the following form:

$$(\rho\, Cp)_{nf}\left(v_r \frac{\partial T}{\partial r} + v_z \frac{\partial T}{\partial z}\right) = \frac{1}{K_{nf}}\left(\frac{1}{r}\frac{\partial}{\partial r}\left(\frac{\partial T}{\partial r}\right) + \frac{\partial^2 T}{\partial z^2}\right) \qquad (15)$$

5. Results and discussion

5.1 A Scanning electron microscope (SEM)

The FE-SEM device's high resolution was used to analyze the morphology of TiO$_2$, CuO, and GNP nanoparticles in Figure 4 (a, b, and c). The images reveal distinct morphologies for CuO and TiO$_2$ particles; CuO nanoparticles exhibit irregular and non-circular shapes, whereas TiO$_2$ nanoparticles display a circular morphology. According to the figures, the particle sizes obtained for the CuO and TiO$_2$ samples are roughly 30 and 30-50 nm, respectively. Graphene nanoplates (GNP) are a form of graphene consisting of multiple layers stacked together, with each sheet typically a few nanometers thick.

5.2 Thermophysical properties of nanofluid

Figure 5 shows that adding nanoparticles to a base fluid (distilled water) changes its physical properties. These effects depend largely on factors such as the type of nanoparticles, their size and concentration, and the properties of the base fluid. Three measurements were made for each sample at every temperature. The average values of the three measures were given. These experiments were repeated at four temperatures (25, 35, 45, and 55) °C. The results of distilled water and nanofluids are shown in Table 2.

It was observed that the highest density of the prepared nanofluids was that of CuO/water nanofluid, and the reason was that copper oxide nanoparticles have a higher density than other nanoparticles used. The maximum liquid density value achieved was 16.36% at 25 °C and 0.003 vol.%. These results are consistent with the studies conducted by Megatif et al., [21].
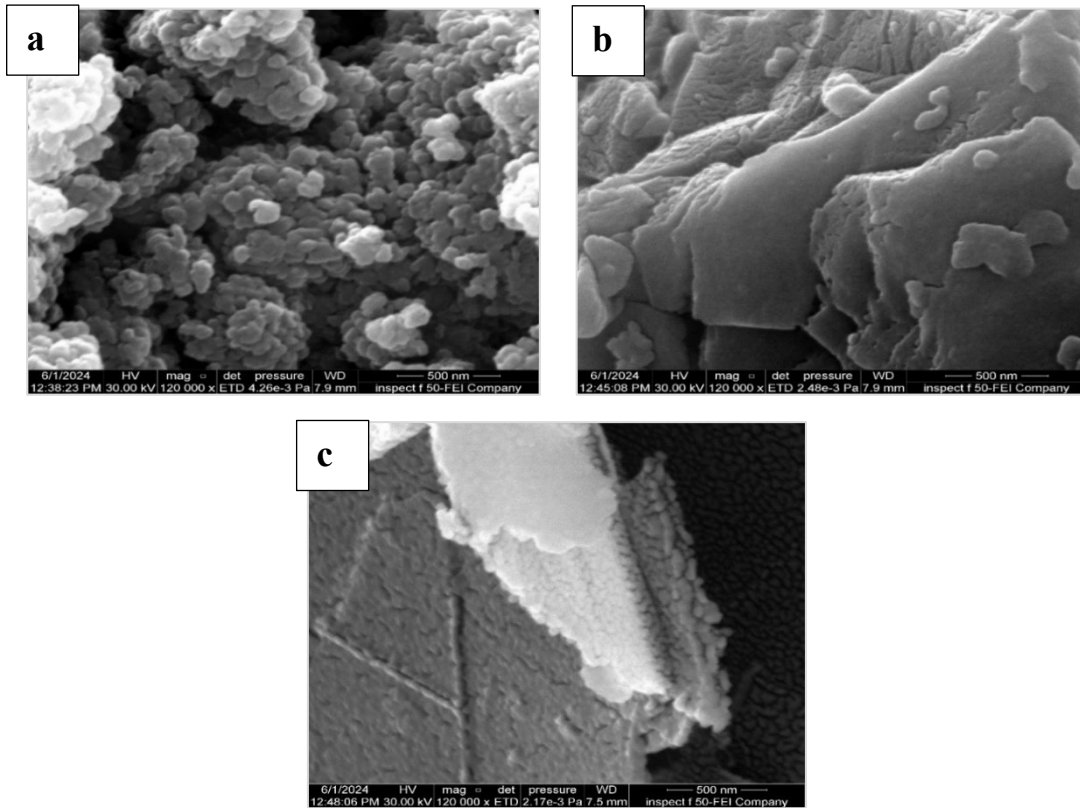
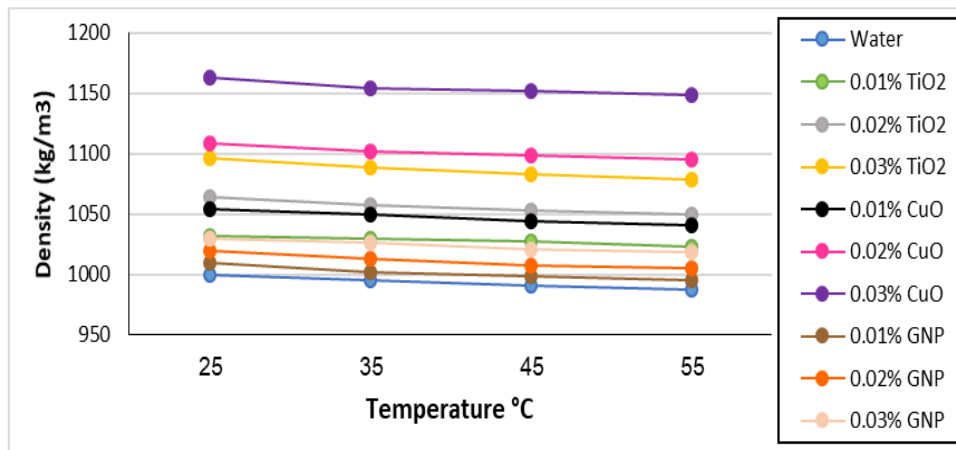**Figure 4:** SEM images of nanoparticles at (500nm) for a) TiO$_2$, b) CuO, and c) GNP

Figure 5: Effect of nanofluid concentration on density vs. temperature for different nanoparticles

Table 2: Variation of the nanofluid and thermo-physical properties at different temperatures.

Samples	Density (kg/m³)	Specific heat (J/kg.k)	Viscosity (kg·m⁻¹·s⁻¹)	Thermal conductivity (W/m·K)
Thermophysical properties at (25 °C)				
Water	999.989	4188	0.0016	0.610
0.01%TiO_2	1032.289	4045.687	0.00164	0.645
0.02%TiO_2	1064.589	3912.01	0.00168	0.672
0.03%TiO_2	1096.889	3786.206	0.00172	0.698
0.01%CuO	1054.549	3965.892	0.00165	0.717
0.02%CuO	1109.109	3765.636	0.00171	0.733
0.03%CuO	1163.669	3584.159	0.00174	0.765
0.01%GNP	1010.009	4119.358	0.00166	0.802
0.02%GNP	1020.029	4052.064	0.00173	0.847
0.03%GNP	1030.049	3986.08	0.00181	0.874
Thermophysical properties at (35 °C)				
Water	995.87	4212.11	0.00159	0.627
0.01%TiO_2	1029.32	4084.32	0.00163	0.672
0.02%TiO_2	1057.48	3915.47	0.00165	0.699
0.03%TiO_2	1088.92	3789.71	0.00169	0.724
0.01%CuO	1049.55	3967.88	0.00162	0.751
0.02%CuO	1101.67	3768.85	0.00168	0.778
0.03%CuO	1154.71	3586.26	0.00171	0.792
0.01%GNP	1002.45	4122.38	0.00162	0.828
0.02%GNP	1013.62	4055.81	0.00171	0.875
0.03%GNP	1026.92	3989.12	0.00179	0.897
Thermophysical properties at (45 °C)				
Water	991.43	4218.35	0.00154	0.641
0.01%TiO_2	1027.77	4096.41	0.00160	0.694
0.02%TiO_2	1052.92	3938.51	0.00161	0.718
0.03%TiO_2	1083.21	3813.37	0.00166	0.756
0.01%CuO	1044.76	3992.45	0.00159	0.778
0.02%CuO	1098.81	3793.62	0.00165	0.795
0.03%CuO	1151.62	3611.73	0.00169	0.824
0.01%GNP	998.72	4157.24	0.00157	0.855
0.02%GNP	1008.14	4082.66	0.00168	0.895
0.03%GNP	1021.27	4011.33	0.00176	0.921

The results in Figure 6 demonstrate that the specific heat of the nanofluid samples decreased as the concentration of Nano additives increased. Additionally, it has been noted that specific heat tends to increase with rising temperatures, as reported by Ha and Das [22]. Therefore, the lowest specific heat capacity of the nanofluid CuO/water was when (0.03) of the volumetric concentration was added at a temperature of 25 °C.
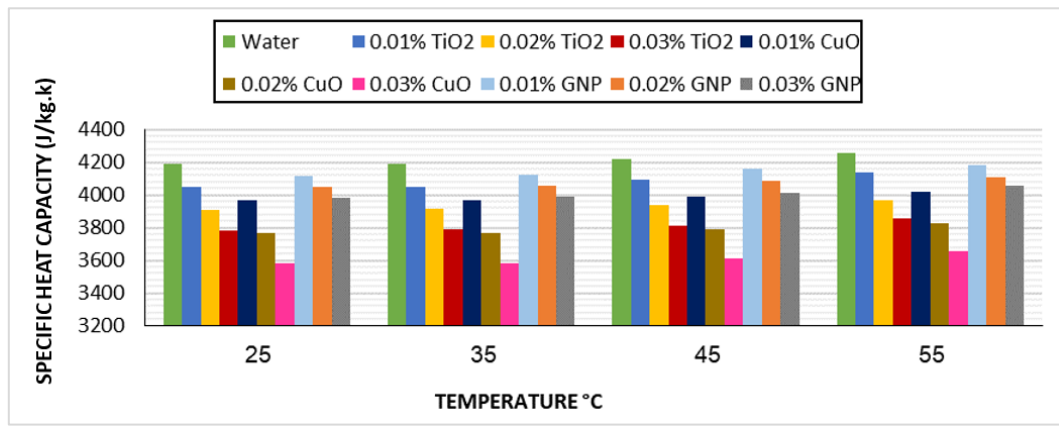
Figure 6: Specific heat capacity of different concentrations of nanofluid with temperature

Nanoparticles can increase the viscosity of the base fluid. This occurs because the particles create resistance to flow due to their interactions with fluid molecules. As shown in Figure 7, the viscosity of nanofluids increases with increasing concentration and decreasing temperature. According to the results, the highest viscosity variation rate occurs with a volume fraction of 0.03 vol% and 25 °C in the experiments conducted by Murshed et al., [23]. Their study revealed that nanofluids containing nanoparticles exhibited lower specific heat than their base fluids. Furthermore, the specific heat values of the nanofluids decreased as the volume fraction of nanoparticles increased.
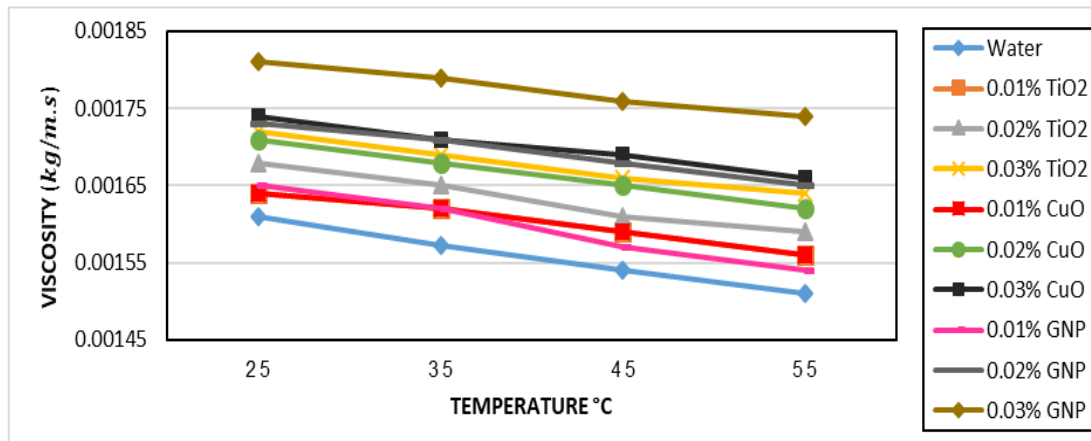
Figure 7: Effect of different types of nanofluid on Dynamic viscosity versus temperature

One of the most notable effects of nanoparticles in fluids is an enhancement in thermal conductivity. For different kinds of nanofluids, including GNP, CuO, and TiO₂, at different temperatures ranging from (25-55) °C. The results showed that adding small amounts of nanoparticles significantly increases thermal conductivity compared to the base fluid. The results also proved that thermal conductivity depends on the type of nanoparticles. The results shown in Figure 8 indicated that thermal conductivity would rise as the temperature rose with a higher concentration of nano-additions, in agreement with Hozien et al., [6].
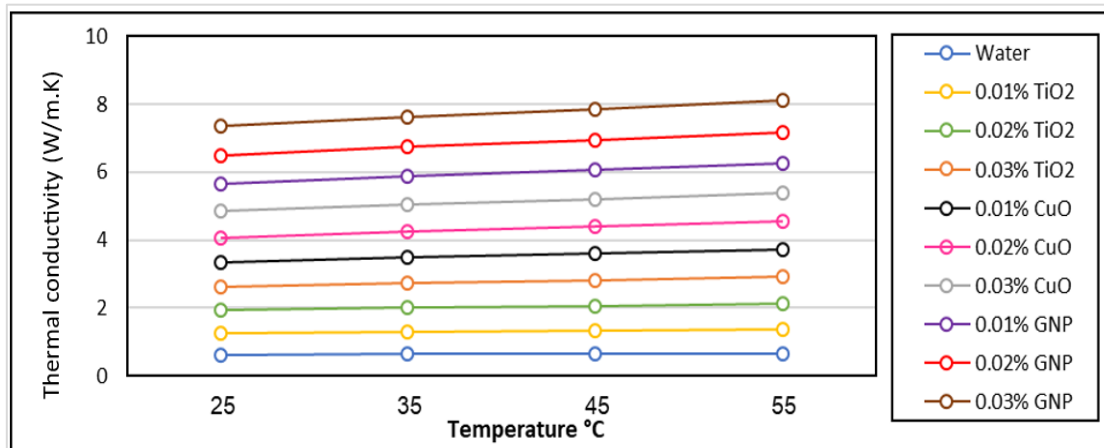

Figure 8: Thermal conductivity of nanofluid with varying temperatures

5.3 Impact of reynold number and concentration nanofluid local heat transfer coefficient

The heat transfer coefficients of nanofluids under flux thermal conditions have been investigated for turbulent flow regimes at different concentrations. Figures 9, 10, and 11 offer how the Reynolds number affects the heat transfer coefficients. Under varying experimental conditions for Reynolds numbers, it has been observed that the heat transfer coefficients rise as the concentration of nanofluid and temperature increase. The findings indicate that the augmentation in the heat transfer coefficients of nanofluids was primarily attributed to the heightened thermal conductivity.

The results show that for nanofluids (TiO_2, CuO, and GNP) at a concentration of 0.03%, there were notable enhancements in the heat transfer coefficients: 12.3, 29.9, and 53.7%, respectively, compared to the base fluid at a Reynolds number of 2579 and 25 °C. This increase in heat transfer coefficient can be attributed to the heightened thermal conductivity resulting from the dispersion of nanoparticles in the nanofluid. The augmented effective thermal conductivity contributes to the overall increase in the heat transfer coefficient. Notably, GNP nanofluids exhibited the most significant enhancement in the heat transfer coefficient compared to CuO and TiO nanofluids, respectively, owing to their superior effective thermal conductivity.

At 35 °C, with a concentration of 0.03% for nanofluids TiO_2, CuO, and GNP, significant enhancements in heat transfer coefficients were observed: 15.5, 32.7, and 59.5%, respectively, compared to the base fluid at a Reynolds number of 2584.

At 45 °C, with a concentration of 0.03% for nanofluids TiO_2, CuO, and GNP, notable enhancements in heat transfer coefficients were achieved: 18.14, 34.18, and 60.11%, respectively, compared to the base fluid at a Reynolds number of 2584.
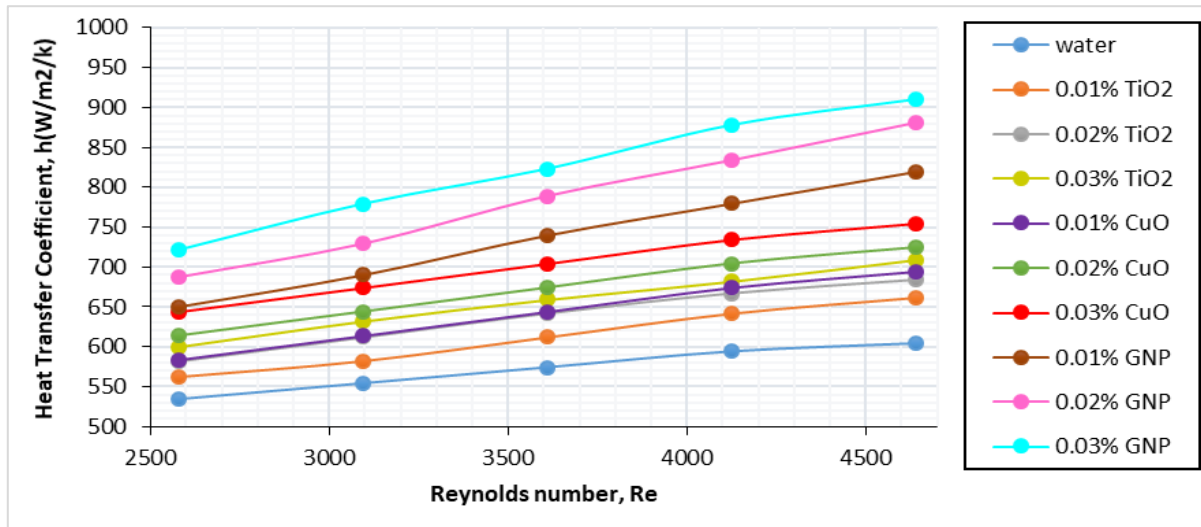

Figure 9: Heat transfer coefficient for different concentrations of nanofluids at 25°C as a function of Reynold number
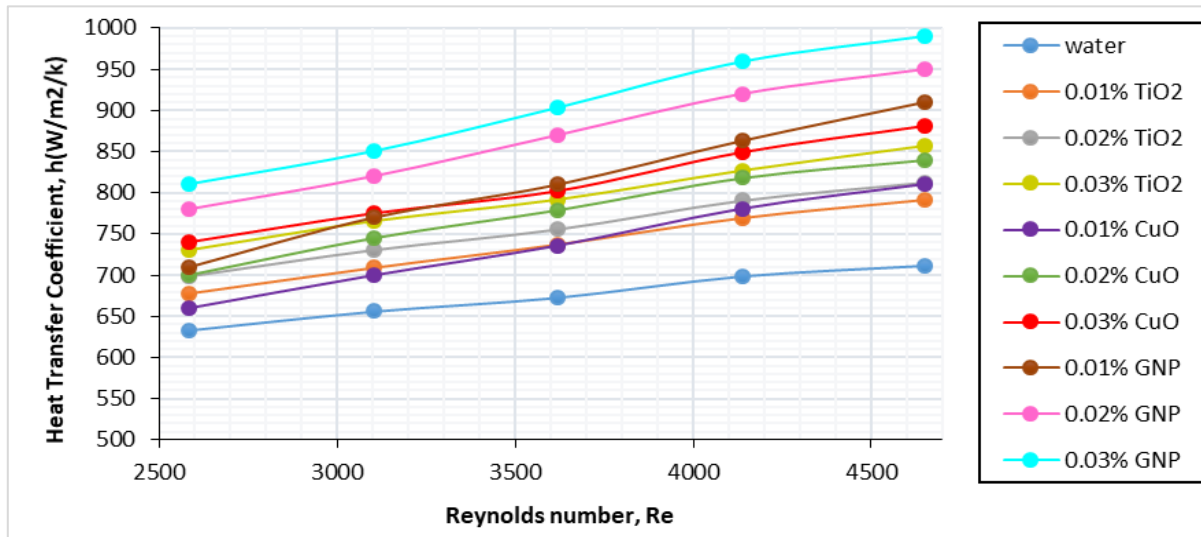

Figure 10: Heat transfer coefficient for different concentrations of nanofluids at 35°C as a function of Reynold number
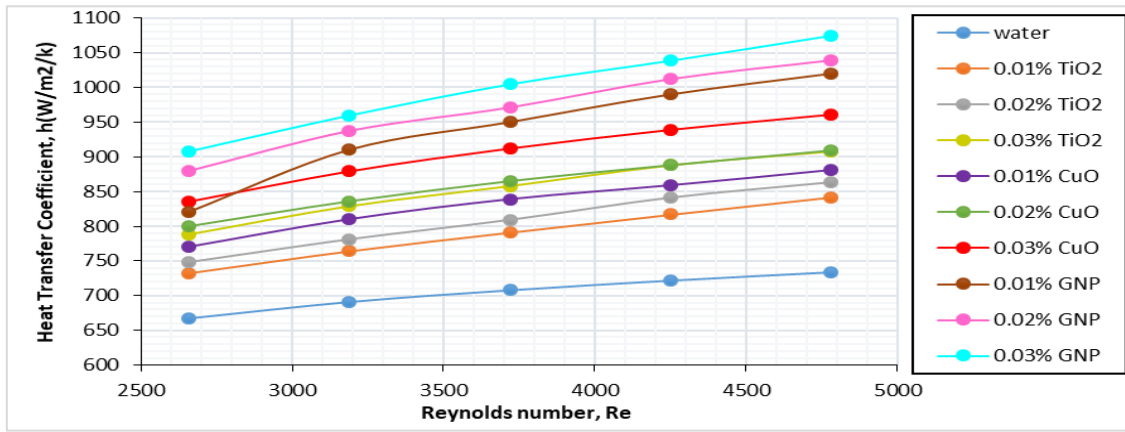
Figure 11: Heat transfer coefficient for different concentrations of nanofluids at 45°C as a function of Reynold number

5.4 Nusselt number

A comparison was made between the experimental data and the correlation established by Dittus Bolter [24]. This relationship was put in the Equation [16]:

$$Nu = 0.023 \, Re^{0.8} pr^{0.4}$$ (16)

As shown in Figures 12, 13, and 14, when the Reynolds number and the concentrations of nanoparticles increase, so does the Nusselt number. Since the nanofluid contains suspended nanoparticles, it needs a lower temperature to reach a specific temperature than distilled water. The increase in Nusselt number observed in nanofluid is linked to various factors, including particle Brownian motion, the thermophysical characteristics of the nanoparticles, and the substantial surface area. Consequently, the heat transfer capacity of nanofluid is expected to improve. This rise in Nusselt number can be ascribed to the advantageous characteristics of nanofluids, such as elevated thermal conductivity and reduced specific heat compared to distilled water [25].
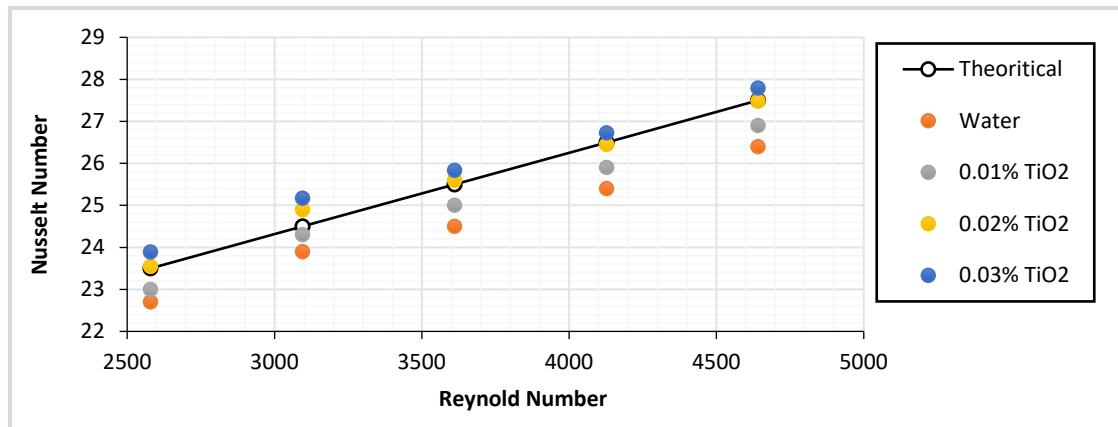

Figure 12: Variation of Nu. With Re. for different concentrations of TiO₂ /water nanofluid
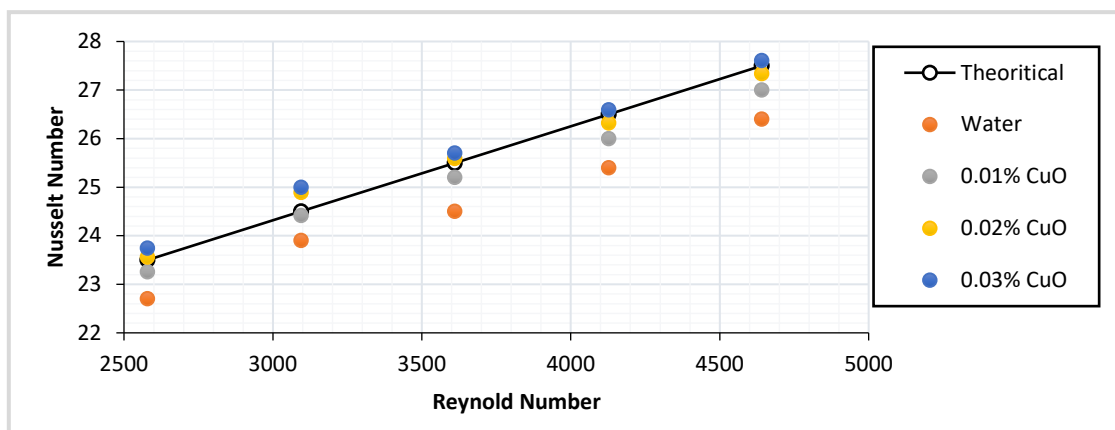

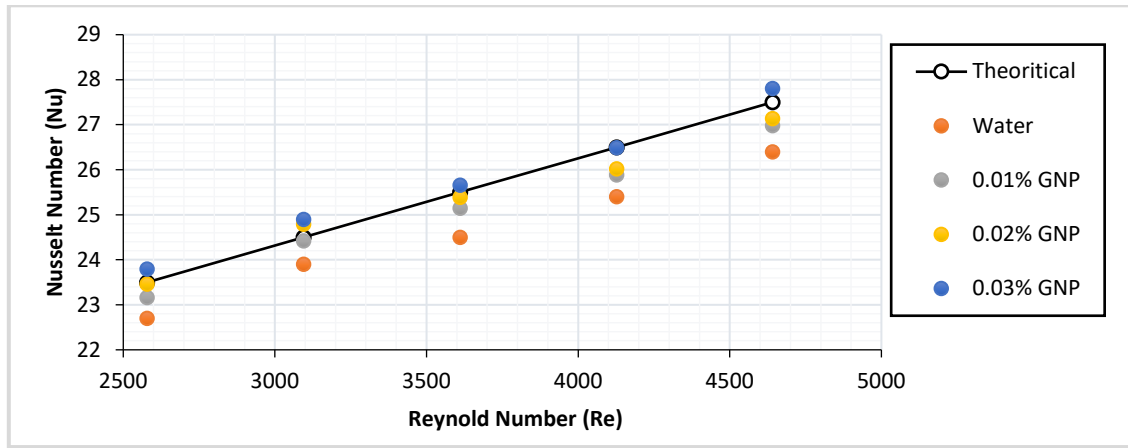**Figure 13:** Variation of Nu. With Re. for different concentrations of CuO/water nanofluid

Figure 14: Variation of Nu. With Re. for different concentrations of GNP/water nanofluid

Thus, at 45 °C and 0.03% volume concentration, the results indicate that the GNP has the highest Nusselt number. CuO and TiO₂ nanofluids come next, with Nu values of 17.8, 11.09, and 8.11%, respectively.

5.5 Friction factor

Figures 15, 16, and 17 show the experimental friction factor of the base fluid and nanofluids in the turbulent flow regime obtained from the experimental results, which agree with Equation (11 and 17). The friction factor of nanomaterials shows higher values than the base fluids. The friction factor rises as the concentration of nanomaterials increases, while it decreases with higher flow rates and Reynolds numbers. This agrees with the results of Sadeghinezhad et al., [16].
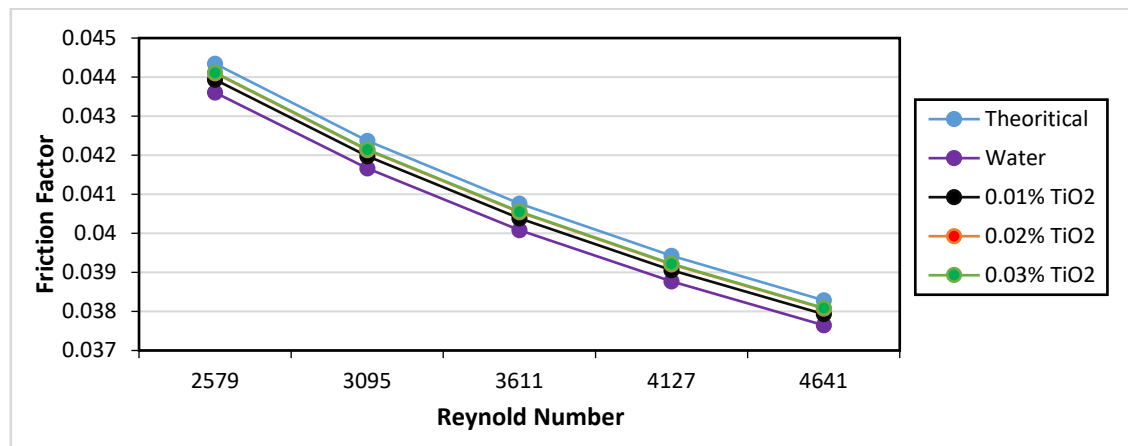
$$f = (0.79 \ln (Re) - 1.64)^{-2} \tag{17}$$

Figure 15: Difference of friction factor with Re. for different TiO₂ /water nanofluid concentrations
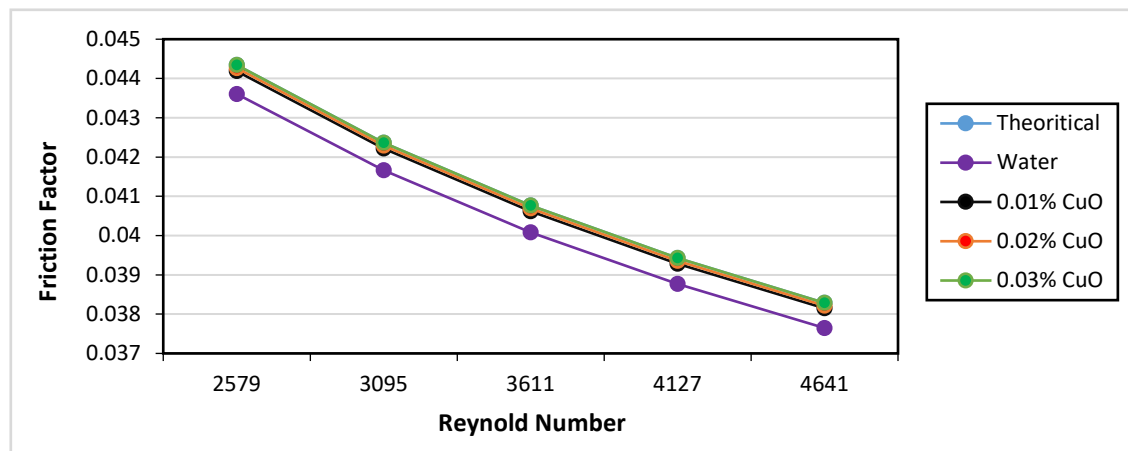

Figure 16: Difference of friction factor with Re. for different CuO /water nanofluid concentrations
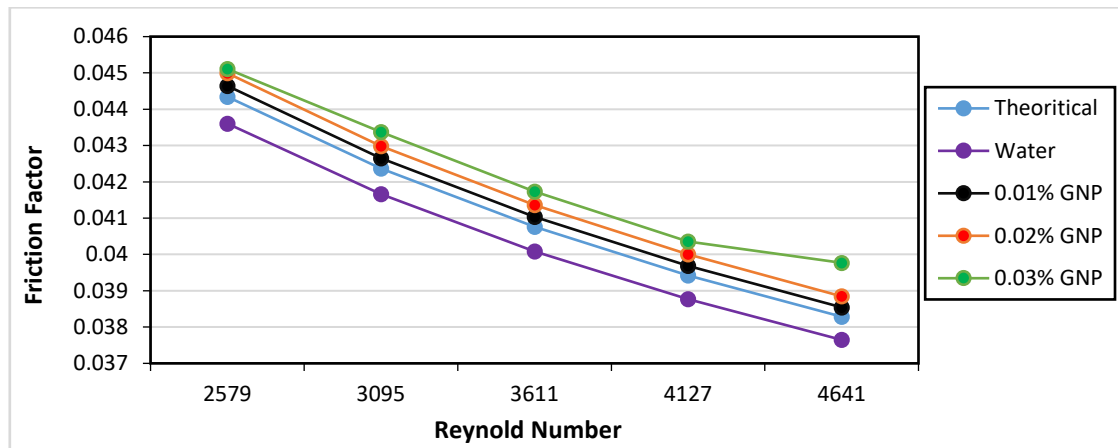
Figure 17: Difference of friction factor with Re. for different GNP/water nanofluid concentrations

5.6 Numerical results

This study's numerical results were produced using COMSOL 5.6, a computational fluid dynamics (CFD) analytical program.

5.6.1 Validation of the model

The predicted and experimental values were compared to evaluate the model's validation. Figure 18 (a and b) illustrates the agreement between experimental and numerical results. Obviously, there are some minor differences between these results. The maximum differences of about 7.2% and 6.7% are seen in predicted and actual temperature values without and with nanofluid, respectively.
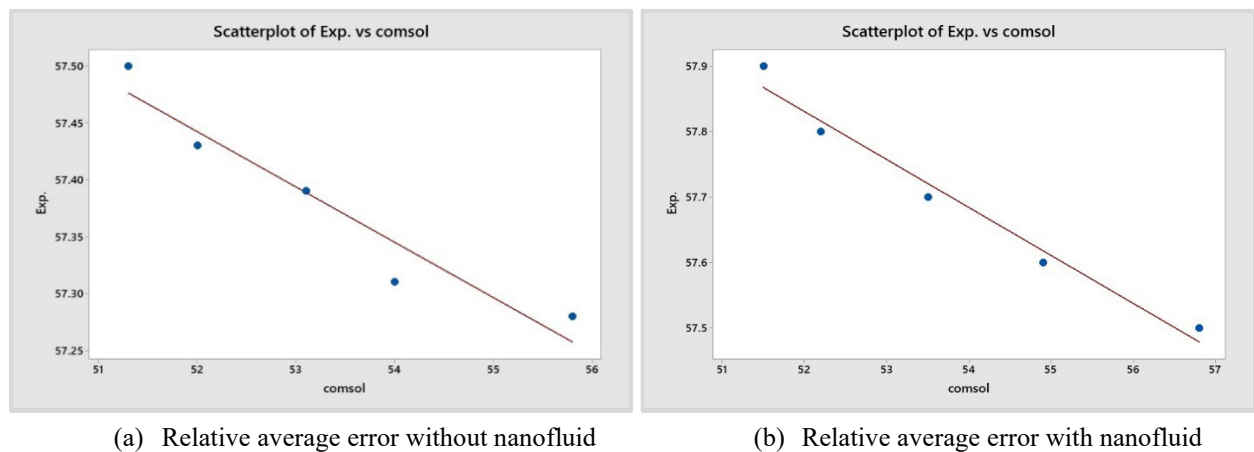

(a) Relative average error without nanofluid

(b) Relative average error with nanofluid

Figure 18: Relative average error with nanofluid and with out nanofluid

5.6.2 Velocity distribution

Figure 19 shows a flow velocity diagram inside a test section tube. The fluid molecules undergo rotational motion as they move through the tube. Maximum velocity occurs at the center of the flow and decreases to zero at the wall. Figure 20 illustrates a cross-section of the velocity distribution of the base fluid in the copper tube.
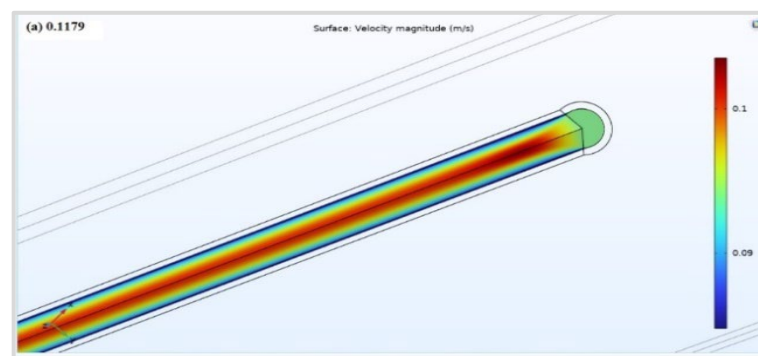

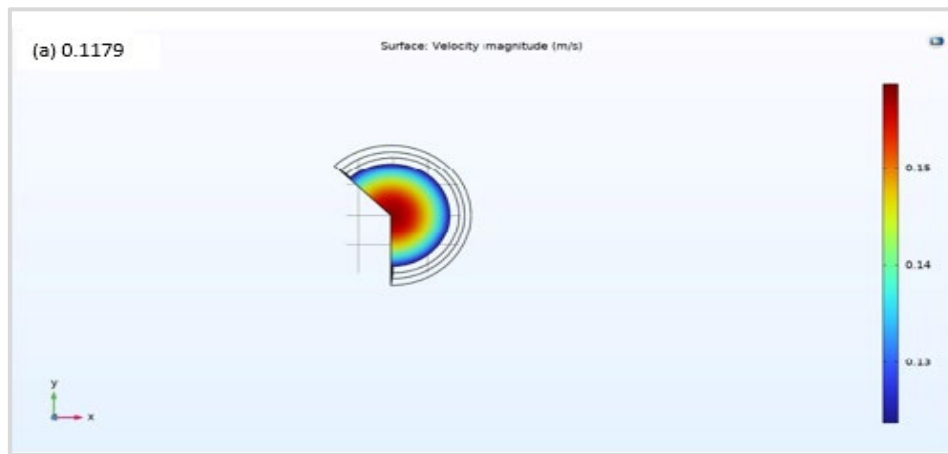**Figure 19:** Velocity distribution of fluid flow along the tube

Figure 20: Front view velocity distribution of fluid in copper tube

5.6.3 Temperature distribution

Figure 21(a, and b) depicts the temperature profile derived from a CFD simulation involving a tube filled with water as the base fluid. A distinct temperature gradient is observable from the tube's center, where temperatures are at their lowest, towards the tube wall, where the color transitions from white to purple. The thermally active zone is concentrated near the inner tube wall, with the purple color intensifying towards the inner surface of the casing, where temperatures peak. Figure 22 shows the trends in temperature distribution inside the tube.

Figure 23 (a and b) illustrate front view of the temperature distribution of both the base fluid and nanofluid in copper tube.
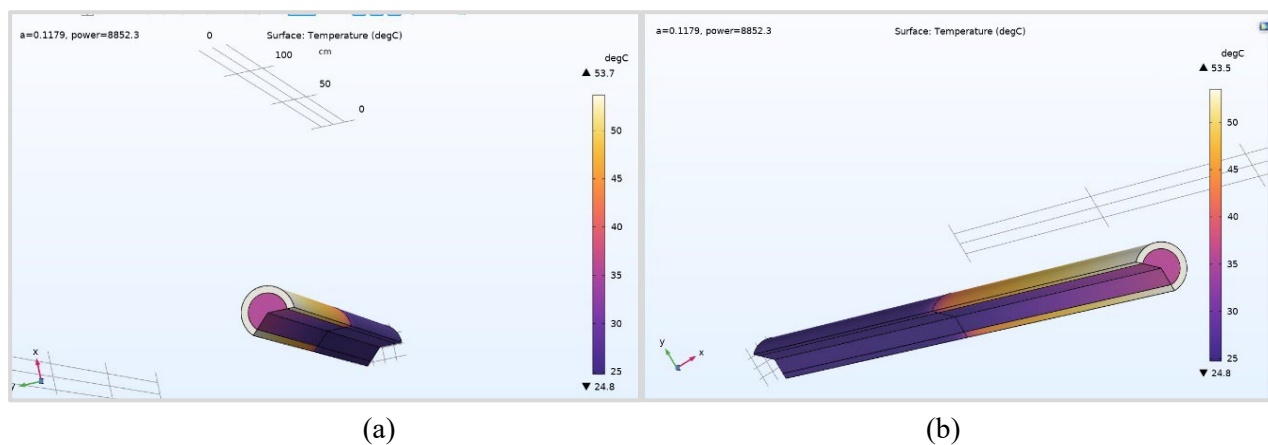

| (a) | (b) |

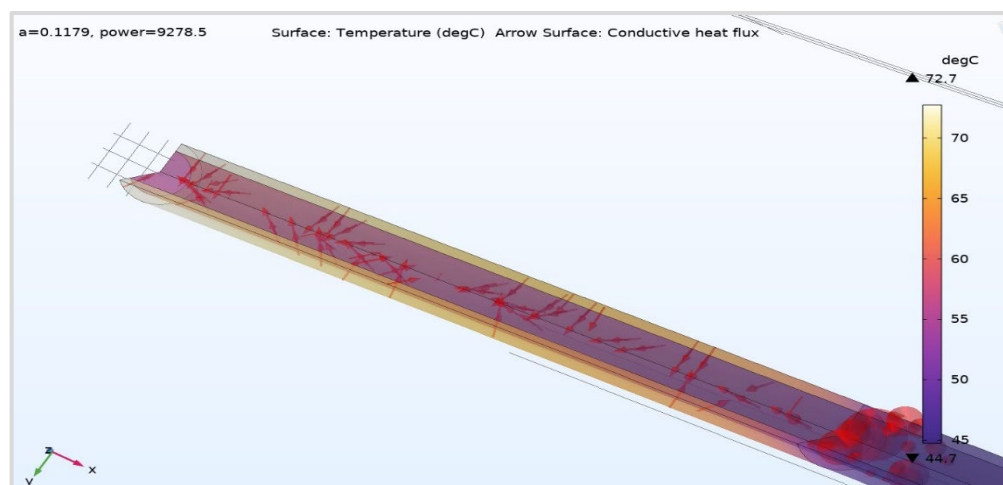**Figure 21:** Temperature profile around the copper tube with water as a working fluid

Figure 22: Temperature distribution trends inside the tube

(a) water as a working fluid   (b) nanofluid as a working fluid
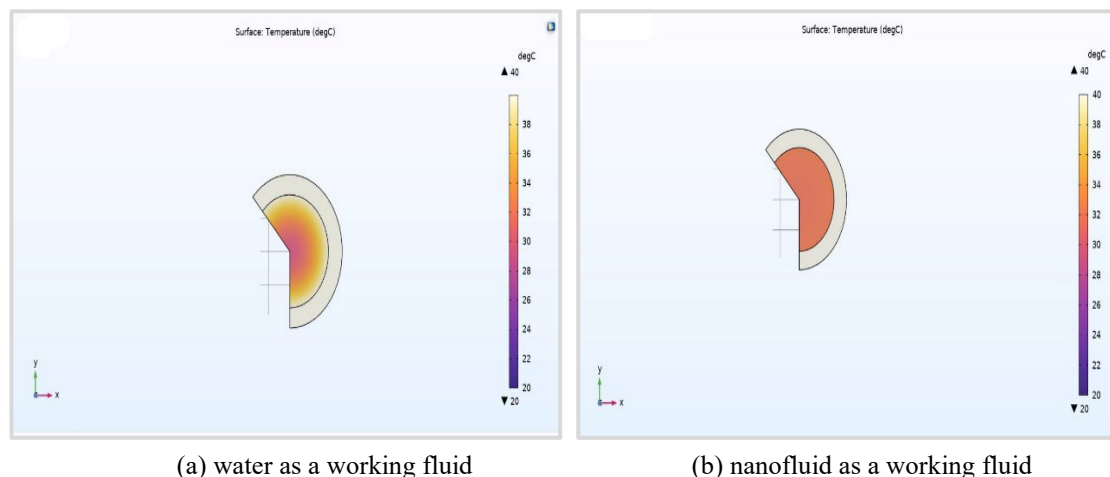
Figure 23: Temperature profile front view of a smooth tube with base fluid and nanofluid

Figure 24 (a and b) shows the temperature distribution radially using different velocities with and without nanofluid.
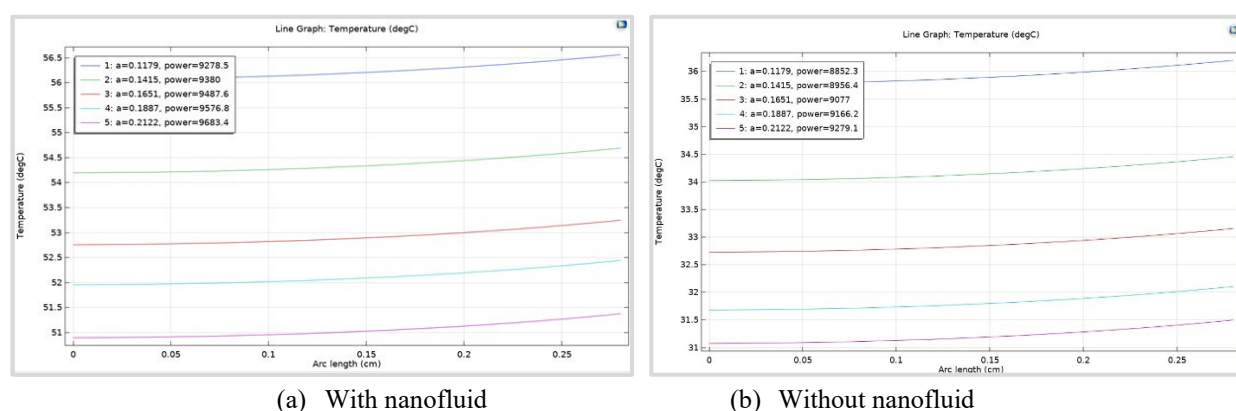

(a) With nanofluid   (b) Without nanofluid

Figure 24: Temperature distribution radially inside the tube using different velocities

6. Conclusion

In this investigation, the thermal properties of nanoparticles (TiO$_2$, CuO, and GNP) dispersed in distilled water were evaluated based on the experimental data from reference [17]. COMSOL Multiphysics numerical simulations were employed to analyze forced convection heat transfer under turbulent flow with varying heat flux boundary conditions within a tube. The study examined heat transfer augmentation attributed to Reynolds number and nanoparticle volume concentration. Nusselt number and friction factor were determined through numerical simulations:

1) According to the results, nanofluids have a better potential to improve heat transmission and are highly appropriate for use in actual heat transfer operations. Convective heat transmission increased by Reynolds number and particle concentration increased. The elevated thermal conductivity of the suspended nanoparticles is the primary cause of the enhanced heat transfer of nanofluids.

2) The incorporation of nanoparticles such as titanium dioxide (TiO$_2$), copper oxide (CuO), and graphene nanoplatelets (GNPs) into heat transfer fluids has been shown to increase both the fluid's thermal conductivity and convective heat transfer coefficients. These improvements can lead to reduced energy consumption, improved system efficiency, and reduced heat exchange systems.

3) The Nusselt number increased with the Reynolds number and heat flow. At a concentration of 0.03% and a flow rate of 5 l/min, the Nusselt numbers for TiO$_2$, CuO, and GNP rose by as much as 8, 11, and 17%, respectively.

4) Carbon-based nanoparticles have a greater effect on improving thermal conductivity when added to the basic fluids. Graphene nanoparticles exhibit high thermal conductivity.

5) The experimental data and the numerical model agree well, which indicates the numerical model's validity for the nanofluids. The maximum differences of about 7.2% and 6.7% are seen in predicted and actual temperature values without and with nanofluid, respectively.

Investigate novel nanomaterials and different types of nanoparticles to create innovative nanofluids. Broaden the application of hybrid nanofluids across various thermal systems to assess their impact on thermal performance and system characteristics. Conduct in-depth studies on the stability of nanofluids to determine optimal concentrations for stability. Utilize a three-dimensional (3D) model in COMSOL Multiphasic simulations to enhance the accuracy and realism of physical analyses.

Nomenclature		List of symbols	
CFD	Computational Fluid Dynamic	ρ	Density
CuO	Copper Oxide	μ	Dynamic Viscosity
GNP	Graphene Nanoplates	Cp	Specific heat capacity
NFs	Nano Fluids	$\emptyset$	Volume concentration
Nu	Nusselt Number		
Re	Reynold Number		
TiO_2	Titanium dioxide		
2D	Two Dimensions		

Author contributions

Conceptualization, **Z. Hussain, J. Ali, H. Majdi, A. Sultan, B. Kadhim,** and **H. Al-Naseri**; data curation, **Z. Hussain,** and **B. Kadhim**; formal analysis, **B. Kadhim**; investigation, **J. Ali**, **H. Majdi**, and **Z. Hussain**; methodology, **J. Ali**, **H. Majdi**, and **H. Al-Naseri**; project administration, **J. Ali**, **Z. Hussain**, and **A. Sultan**; resources, **J. Ali**, **H. Al-Naseri**, and **Z. Hussain**; software, **B. Kadhim**; supervision, **J. Ali**, and **H. Majdi**; validation, **J. Ali**, **Z. Hussain**, and **B. Kadhim**; visualization, **J. Ali**, and **A. Sultan**; writing—original draft preparation, **Z. Hussain**, and **J. Ali**; writing—review and editing, **J. Ali**, **Z. Hussain**, and **A. Sultan**. All authors have read and agreed to the published version of the manuscript.

Funding

Data availability statement

The data that support the findings of this study are available on request from the corresponding author.

Conflicts of interest

The authors declare that there is no conflict of interest.

References

[1] Z. N. Hussain, J. M. Ali, H. S. Majdi, and A. J. Sultan, Study the Convective Heat Transfer Intensification by using Nanotechnology : A Review, Russ. J. Appl. Chem., 97 (2024) 147-168. https://doi.org/10.1134/S1070427224010129

[2] Thermophysical Properties of Complex Materials, Thermophysical Properties of Complex Materials. 2019. https://doi.org/10.5772/intechopen.81990

[3] L. Godson, B. Raja, D. Mohan Lal, and S. Wongwises, Enhancement of heat transfer using nanofluids-An overview, Renewable Sustainable Energy Rev., 14 (2010) 629-641. https://doi.org/10.1016/j.rser.2009.10.004

[4] Z. M. Omara, A. E. Kabeel, and F. A. Essa, Effect of using nanofluids and providing vacuum on the yield of corrugated wick solar still, Energy Convers. Manage., 103 (2015) 965-972. https://doi.org/10.1016/j.enconman.2015.07.035

[5] Z. Guo, A review on heat transfer enhancement with nanofluids, J. Enhanc. Heat Transf., 27 (2020) 1-70. https://doi.org/10.1615/JEnhHeatTransf.2019031575

[6] O. Hozien, W. M. El-Maghlany, M. M. Sorour, and Y. S. Mohamed, Experimental study on thermophysical properties of TiO_2, ZnO and Ag water base nanofluids, J. Mol. Liq., 334 (2021) 116128. https://doi.org/10.1016/j.molliq.2021.116128

[7] M. J. Uddin, K. S. Al Kalbani, M. M. Rahman, M. S. Alam, N. Al-Salti, and I. Eltayeb, Fundamentals of nanofluids: evolution, applications and new theory, International Journal of Biomathematics and Systems Biology, Int. J. Biomath. Syst. Biol., 2 (2016) 1-32.

[8] I. A. Ismail, M. Z. Yusoff, F. B. Ismail, and P. Gunnasegaran, Heat transfer enhancement with nanofluids: A review on recent applications and experiments, AIP Conf. Proc., 2035 (2018). https://doi.org/10.1063/1.5075570

[9] A. A. Hussien, M. Z. Abdullah, N. M. Yusop, M. A. Al-Nimr, M. A. Atieh, and M. Mehrali, Experiment on forced convective heat transfer enhancement using MWCNTs/GNPs hybrid nanofluid and mini-tube, Int. J. Heat Mass Transf., 115 (2017) 1121-1131. https://doi.org/10.1016/j.ijheatmasstransfer.2017.08.120

[10] R. Anand, A. Raina, M. Irfan Ul Haq, M. J. Mir, O. Gulzar, and M. F. Wani, Synergism of TiO_2 and Graphene as Nano-Additives in Bio-Based Cutting Fluid—An Experimental Investigation, Tribol. Trans., 64 (2021) 350-366. https://doi.org/10.1080/10402004.2020.1842953

[11] F. I. Doshmanziari, M. R. Kadivar, M. Yaghoubi, D. Jalali-Vahid, and M. A. Arvinfar, Experimental and Numerical Study of Turbulent Fluid Flow and Heat Transfer of Al_2O_3/Water Nanofluid in a Spiral-Coil Tube, Heat Transfer Eng., 38 (2017) 611-626. https://doi.org/10.1080/01457632.2016.1200380

[12] M. Mahmoudi, M. R. Tavakoli, M. A. Mirsoleimani, A. Gholami, and M. R. Salimpour, Experimental and numerical investigation on forced convection heat transfer and pressure drop in helically coiled pipes using TiO_2/water nanofluid, Int. J. Refrig., 74 (2017) 627-643. https://doi.org/10.1016/j.ijrefrig.2016.11.014

[13] M. Afrand, N. Sina, H. Teimouri, A. Mazaheri, M. R. Safaeiet, et al, Effect of Magnetic Field on Free Convection in Inclined Cylindrical Annulus Containing Molten Potassium, Int. J. Appl. Mech., 7 (2015) 1-16. https://doi.org/10.1142/S1758825115500520

[14] H. S. Majdi, H. A. Alabdly, M. F. Hamad, B. O. Hasan, and M. M. Hathal, Enhancement of Heat Transfer using Aluminum Oxide Nanofluid on Smooth and Finned Surfaces with COMSOL Multiphysics Simulation in Turbulent Flow, Al-Nahrain J. Eng. Sci., 22 (2019) 44-54. https://doi.org/10.29194/njes.22010044

[15] A. Sivakumar, N. Alagumurthi, and T. Senthilvelan, Experimental investigation of forced convective heat transfer performance in nanofluids of Al_2O_3/water and CuO/water in a serpentine shaped micro channel heat sink, Heat Mass Transf. und Stoffuebertragung, 52 (2016) 1265-1274. https://doi.org/10.1007/s00231-015-1649-5

[16] E. Sadeghinezhad, H. Togun, M. Mehrali, P. S. Nejad, S. T. Latibari, et al., An experimental and numerical investigation of heat transfer enhancement for graphene nanoplatelets nanofluids in turbulent flow conditions, Int. J. Heat Mass Transf., 81 (2015) 41-51. https://doi.org/10.1016/j.ijheatmasstransfer.2014.10.006

[17] B. C. Pak and Y. I. Cho, Hydrodynamic and heat transfer study of dispersed fluids with submicron metallic oxide particles, Exp. Heat Transf. an Int. J., 11 (1998) 151-170. http://dx.doi.org/10.1080/08916159808946559

[18] R. B. Bird, Transport phenomena, Appl. Mech. Rev., 55 (2002) R1–R4. https://doi.org/10.1115/1.1424298

[19] A. M. Hussein, Thermal performance and thermal properties of hybrid nanofluid laminar flow in a double pipe heat exchanger, Exp. Therm. Fluid Sci., 88 (2017) 37–45. https://doi.org/10.1016/j.expthermflusci.2017.05.015

[20] K. P. Venkitaraj, S. Suresh, T. Alwin Mathew, B. S. Bibin, and J. Abraham, An experimental investigation on heat transfer enhancement in the laminar flow of water/TiO_2 nanofluid through a tube heat exchanger fitted with modified butterfly inserts, Heat Mass Transf., 54 (2018) 813–829.

[21] L. Megatif, A. Ghozatloo, A. Arimi, and M. Shariati-Niasar, Investigation of Laminar Convective Heat Transfer of a Novel Tio2-Carbon Nanotube Hybrid Water-Based Nanofluid, Exp. Heat Transf., 29 (2016) 124–138. https://doi.org/10.1080/08916152.2014.973974

[22] Rv. S. Ha and D. K. Das, Specific heat measurement of three nanofluids and development of new correlations, 2009.

[23] S. M. S. Murshed, K. C. Leong, and C. Yang, Investigations of thermal conductivity and viscosity of nanofluids, Int. J. Therm. Sci., 47 (2008) 560–568.

[24] F. W. Dittus, Heat Transfer in Automobile Radiators of the Tubular Type, Univ. Calif. Publ. Eng., 1930.

[25] H. Yarmand, S. Gharehkhani, G. Ahmadi, S. Shirazi, S. Baradaran, et al., Graphene nanoplatelets-silver hybrid nanofluids for enhanced heat transfer, Energy Convers. Manag., 100 (2015) 419–428. https://doi.org/10.1016/j.enconman.2015.05.023